# FAST TWO-DIMENSIONAL DIFFRACTION MODELLING FOR MOBILE RADIO PROPAGATION PREDICTION IN URBAN MICRO-CELLULAR ENVIRONMENTS

W. Zhang [*] , J. Lähteenmäki [2] , P. Vainikainen [3] , H. El-Sallabi [4]

[*] Helsinki University of Technology, Institute of Radio Communications/Radio Laboratory,
P. O. Box 3000, FIN-02015 HUT, Finland, WZH@radio.hut.fi

[3] Pertti.Vainikainen@hut.fi

[4] HEL@radio.hut.fi

[2] VTT Information Technology, P. O. Box 1202, FIN-02044 VTT, Finland, Jaakko.Lahteenmaki@vtt.fi

## ABSTRACT

The paper presents fast two-dimensional (2-D) diffraction modelling in the horizontal plane for site-specific propagation prediction in urban micro-cellular environments. Comparison with measurements and simulation of published results validate the 2-D modelling that significantly reduces the computation time and overcomes the limitation and difficulty of existing techniques for multiple building diffraction. The modelling makes three contributions which are 1) extension of an expression for multiple building forward diffraction and use of the extended formulation, 2) equivalent source technique for parallel-street multiple diffraction and 3) inclusion of reflections from curved surfaces of street building corners. Additional comparisons of three-dimensional model prediction with measurements for an urban line-of-sight environment place the work in a more complete context. The results show that an increase in the number of rays may not enhance the accuracy of ray-tracing model prediction.

## INTRODUCTION

It is necessary and important to develop efficient propagation prediction tools for the design and development of future broadband communication systems. The lengthy time spent in ray-trace computation is a major existing problem with mobile radio propagation prediction for urban micro-cellular environments [1-3]. The use of two-dimensional (2-D) methods in a horizontal plane appears to be a solution for site-specific prediction for both transmitter and receiver lower than the surrounding buildings [1, 4, 5]. It was seen that fast 2-D methods which do not require a building height database can provide good, at least acceptable, accuracy in most cases. However, further studies on multiple diffraction are required, because after the first diffraction there is a difficulty in determining and successfully using the second and later diffraction, especially for parallel streets [2-4]. It is difficult to select a formulation for amplitude factors and distance parameters from different formulations used in the technical literature. Moreover, the uniform geometrical theory of diffraction (UTD) [6] itself may become incorrect when multiple diffraction edges modelling the buildings are in the transition zone of the preceding edges. Incidentally, it is necessary to include the reflection rays from curved surfaces of street building corners, which have larger amplitudes and may play important role in total signal reception in the shadow, i.e. out-of-sight, regions.

This work focuses on 2-D diffraction modelling to overcome the limitation and difficulty of existing diffraction formulations. In particular, the 2-D diffraction modelling makes an extension of the expression of [7] for multiple forward diffraction and an equivalent source simplification for parallel street multiple diffraction, as well as the inclusion of the reflection rays from convex or concave surfaces of street building corners. To validate the three new efforts, comparisons of model predictions with measurements are made, along with simulation of published measurements and predictions.

To place the paper in proper perspective, the measurement set-up is first summarised. Descriptions of 2-D diffraction modelling are given then. To make a more complete context of the work, a comparison of three-dimensional (3-D) ray-trace model prediction with measurements in an urban line-of-sight (LOS) environment is included. The salient points of the entire work are described in the following.

## MEASUREMENT SET-UP

A number of propagation measurements were performed in an area in the city centre of Helsinki, Finland, shown in Fig 1. The base station (BS) was placed on a balcony and the mobile station (MS) moved with a car. Both stations are much lower than the surrounding buildings. The key parameters of the measurement system are listed in Table 1. The BS antennas were fixed towards the main street from BS to D and the 3-dB main lobe of radiation patterns ranges about from $-20^{\circ}$ to $20^{\circ}$ off their pointing direction in both horizontal and vertical plane. The measured signal strengths were converted into path loss, in dB, defined by the ratio of radiated to received power for isotropic antennas. The estimated root mean square error for position is 3 meters.

## TWO-DIMENSIONAL DIFFRACTION MODELLING

The total path loss $L_t$ in dB is formulated as

$$L_t = L_{1v} - 20\log_{10}\left|1+\sum_{i=2}^{M}\frac{E_{iv}}{E_{1v}}\right| \quad (1)$$

where $L_{1v}$ is the path loss of a multiple diffraction ray, that was expressed in [8], and $E_{iv}$ is the electric field of rays for vertical polarisation transmission and reception applying to most cases of mobile radio and this work. This work uses about $M = 8$ dominant rays which appear adequate for model prediction in urban street grid environments as indicated by Fig 1, where the base station was in the centre of the main street. When a mobile station is at a side street, e.g. street AOB, multiple diffraction from street building corners on both sides of a main street contributes to the total received signal.

As a first effort, a multiple diffraction ray is determined by the multiplication of a ratio $|E_n / E_0|$ of an extended formulation and a single diffraction field by a street building corner (numbering $n$) for spherical-wave incidence from the base station. This formulation extends the applicable region of the expression of $|E_n / E_0|$ of [7] and additionally accounts for a base station placed on, or very close to, either side of a main street. As defined in [7], $E_0$ and $E_n$ are the field magnitude of an incident plane wave and its corresponding total field at the local edge modelling the street building corner. The buildings along side streets are considered as rows of knife edges with an equal spacing $d$ and the rows are numbered. For the row number $n = 1$, it is unnecessary to include multiple diffraction. The extended formulation for multiple building forward diffraction is presented in the Appendix.

As a second effort, an equivalent source technique is introduced and used for parallel-street multiple diffraction problems, similar to the image source [3] for reflections. It is the key point that an equivalent source must keep the shadow boundaries for the mobile and the same amount power of a direct wave on the edge just before the first parallel street (e.g. a street from B to C of Fig 1 results for which were already presented [5]). For such and similar configurations, the ray-tracing techniques used appear unable to reduce up to 20-dB difference between measurements and predictions as seen in Fig. 8 of [3] and Fig. 16 of [4]. The equivalent source technique makes the parallel street propagation predictable by using a simple yet accurate method which has been successful for side-street environments. Applying the new formulation of $|E_n / E_0|$ and including more rays, this technique appears efficient for propagation predictions for the mobile terminals along a number of parallel streets and has more applications.

As a third effort of this work, rays from reflections at curved surfaces of street building corners are derived and included. For example, reflections from a building corner at the first cross street junction of Fig 1 take place. A normal vector of a tangential plane of the concave surface varies in a range, nearly from $-\hat{y}$ to $-\hat{x}$ towards the base station. A reflection angle off such a normal vector may be estimated by a half of the angle between the incoming (from BS) and forgoing (to MS) directions of the ray, if MS is in the $-y$ region of the side street. The reflection can be calculated by using the well-known Fresnel reflection coefficient. Rays from this and similar reflections may involve other processes such as multiple diffraction formulated as $|E_n / E_0|$ and single or multiple reflection.

## COMPARISONS AND SIMULATION

An example of comparisons of 2-D model prediction with measurements is presented in Fig 2. Using the new multiple diffraction formulation for grazing incidence, the equivalent source technique produces results in the streets from F to J and from F to G. Near the junction O of side street AOB, contributions of multiple-reflection rays from street building corners are significant.

Comparisons of 3-D ray-trace prediction in an LOS region with measurements are presented in Fig 3 and Table 2. The four- and eight-ray model predictions are obtained by adding two reflection rays to existing two- and six-ray [9] models, respectively. One is a single reflection from a transverse wall at the street junction D. Another is a double reflection from the wall and the ground. It is interesting to see that the root mean square error $\Delta_{rms}$ is smallest for the two-ray model.

Simulations of published results [2-4] spent much less computation time and provide an improvement over the predictions of Fig. 16 of [4]. Derived from the equivalent source technique for parallel-street multiple diffraction, the simulation reduces that difference between measurements and predictions and appears in the order of that measurement. Presentations of the simulations are omitted.

## CONCLUSIONS

Three new efforts are validated comparing with measurements and simulating published results. They are the extension of an expression for multiple forward diffraction and use of the extended formulation, an equivalent source technique for parallel street multiple diffraction and the inclusion of reflections from curved surfaces of street building corners. The entire 2-D diffraction modelling significantly reduces the computation time and overcomes the limitation and difficulty of existing techniques for multiple building diffraction. The comparison of 3-D model prediction with measurements for an urban LOS environment makes a more complete context of the work. The results indicate that an increase in the number of rays may not enhance the accuracy of ray-tracing model prediction.

## APPENDIX

The appendix introduces the extended formulation of $|E_{n+1} / E_0|$ for multiple forward diffraction. Let $\lambda$ be the wavelength, $k$ be the wave-number, $\alpha$ be the azimuth angle off the BS antenna pointing direction $\hat{x}$ and $g = \sin\alpha\sqrt{d/\lambda}$. In the range of $g > 0$, the ratio of $|E_{n+1} / E_0|$ [7] is written as

$$\frac{E_{n+1}}{E_0} = 1 + \frac{D_{s,h}}{\sqrt{d}} \exp\left[-jkd(1-\cos\alpha)\right] \frac{1 - \left(D^c_{s,h} \exp\left[-jkd(1-\cos\alpha)\right] / \sqrt{d}\right)^n}{1 - D^c_{s,h} \exp\left[-jkd(1-\cos\alpha)\right] / \sqrt{d}} \tag{2}$$

$$D_{s,h} = \frac{-\exp(-j\pi/4)}{2\sqrt{2\pi k}} \left[ \frac{F(X)}{\sin(\alpha/2)} \mp \frac{1}{-\cos(\alpha/2)} \right] \tag{3}$$

$$F(X) = \sqrt{\pi X}\, \exp\left(j\pi/4 + jX\right) - 2j\sqrt{X}\, \exp\left(jX\right) \int_0^{\sqrt{X}} \exp\left(-j\tau^2\right) d\tau \tag{4}$$

$$\sqrt{X} = \sqrt{2kd}\,|\sin(\alpha/2)| \tag{5}$$

$$D^c_{s,h} = \frac{-\exp(-j\pi/4)}{2\sqrt{2\pi k}} \left[ -\sqrt{\pi k d} \cdot \exp\left(j\pi/4\right) \mp (-1) \right] \tag{6}$$

where subscripts '$s$' and '$h$' of UTD diffraction coefficients $D_{s,h}$ and $D^c_{s,h}$ denote soft and hard boundaries, respectively. And they take signs '–' and '+' on the right-hand side of eqns. 3 and 6. The soft boundary corresponds to vertical polarisation transmission and reception in the horizontal plane. The transition function $F(X)$ can be approximated by $F(X) \approx \sqrt{\pi X}\, \exp(j\pi/4 + jX)$ for $X < 10^{-3}$ and $F(X) \approx 1$ for $X > 10$.

For $0 \le g \approx \alpha\sqrt{d/\lambda} < 0.1$ including the grazing incidence of $\alpha \to 0$, the extension for $|E_{n+1} / E_0|$ is expressed as

$$\frac{E_{n+1}}{E_0} = 1 + \frac{D_{s,h}}{\sqrt{d}} \exp\left[-jkd(1-\cos\alpha)\right] \frac{1 - 1/\sqrt{3n+1}}{-D_{s,h}|_{\alpha=0} / \sqrt{d}} \tag{7}$$

$$D_{s,h}|_{\alpha=0} = \frac{-\exp(-j\pi/4)}{2\sqrt{2\pi k}} \left[ \sqrt{2\pi k d} \cdot \exp\left(j\pi/4\right) \mp (-1) \right]. \tag{8}$$

Here, the simple expression $1/\sqrt{3n+1}$ by Walfisch and Bertoni [10] is used. It approximates $\Gamma(n+1/2) / \left(\sqrt{\pi} n!\right)$ derived in [11] valid for both hard and soft boundaries. Due to $kd >> 1$ and $\alpha$ small leading to $\cos(\alpha/2) \sim 1$, the second term on the right-hand side of eqns. 3, 6 and 8 is negligibly small compared with the first term. Therefore, eqns. 7 and 2 are dependent on and insensitive to the polarisation (type of boundaries). Since $d$ ranges about from 30 to 100 meters, $kd >> 1$ is naturally satisfied at UHF (300 MHz-3 GHz) and microwave frequencies used in mobile communications.

Numerical comparisons of eqns. 2 and 7 of hard boundary with formulations of [12-14] are presented in Fig 4, at $d/\lambda = 200$ for $g = \sin\alpha\sqrt{d/\lambda}$ from 0 to 0.494. At $g = 0$, it is seen that $1/\sqrt{3n+1}$ of eqn. 7 indeed approaches $\Gamma(n+1/2)/\left(\sqrt{\pi}n!\right)$ which all other formulations take. Formulations by Saunders and Bonar [12] and by Juan-Llacer and Cardona [13] give nearly same numerical results. Results of Xia and Bertoni formulation are computed from equation (17) of [14]. This series solution is rapidly convergent for $g$ small and almost the same numerical results as those of formulations in [12, 13] are generated. Numerical results of eqn. 2 for $g \geq 0.1$ and of eqn. 7 for $g < 0.1$ agree with those of other formulations.

To further examine eqns. 7 and 2 for $\alpha \approx 2\sin(\alpha/2)$ small and $g \approx \alpha\sqrt{d/\lambda}$ small, approximate eqn. 4 by

$$F(X) \approx \left[\sqrt{\pi X} - 2X\exp\left(j\pi/4\right)\right]\exp\left(j\pi/4 + jX\right) \tag{9}$$

for $X \approx \pi g^2$ small [6]. One thus derives from eqn. 3

$$D_{s,h}/\sqrt{d} \approx -1/2 + g\exp\left(j\pi/4\right). \tag{10}$$

As a result, eqn. 2 can be approximated by

$$E_{n+1}/E_0 \approx 0.227 + 1.55g\exp\left(j\pi/4\right) \tag{11}$$

for $g \geq 0.1$ and $n \geq 6$. And eqn. 11 further becomes

$$E_{n+1}/E_0 \sim 1.55g \tag{12}$$

for $g > 0.146$. Similarly, eqn. 7 can be approximated by

$$E_{n+1}/E_0 \approx 1/\sqrt{3n+1} + 2g\left(1 - 1/\sqrt{3n+1}\right)\exp\left(j\pi/4\right) \tag{13}$$

and approaches

$$E_{n+1}/E_0 \sim 2g \tag{14}$$

for $n >> 1$ or $n \to \infty$. The settled field $Q$ by equation (14) of Walfisch and Bertoni [10] is written as

$$Q \approx 0.1\left[\frac{\alpha\sqrt{d/\lambda}}{0.03}\right]^{0.9} \tag{15}$$

for $\alpha\sqrt{d/\lambda}$ ranging about from 0.02 to 0.4. It can be further expressed by

$$Q \approx 2.35g^{0.9}. \tag{16}$$

It is interesting to see that eqn. 16 is comparable with asymptotic expressions of eqns. 14 and 12.

For $n = 6$, eqn. 13 becomes

$$E_{n+1}/E_0 \approx 0.229 + 1.54g\exp\left(j\pi/4\right). \tag{17}$$

Incidentally, eqn. 2 smoothly approaches eqn. 7 when $g \to 0.1$ for $n \leq 6$. Also, eqn. 7 avoids the difficulty of eqn. 16 and is valid at $\alpha\sqrt{d/\lambda} \to 0$. Agreeing with other formulations [12-14], the extended formulation of eqns. 7 and 2 significantly reduces the computation time. Both eqns. 7 and 2 additionally apply to soft boundary. This enables the application in the horizontal plane for vertical polarisation transmission and reception.

**ACKNOWLEDGEMENT**

This work was supported by the Academy of Finland and by Technology Development Centre (TEKES), Finland. The authors would like to thank Prof. A. Räisänen for his encouragement.

**REFERENCES**

1 Liang G and Bertoni H L, Review of ray modeling techniques for site specific propagation prediction, 1997, Wireless Communications TDMA versus CDMA, Edited by Glisic S G and Leppänen P A, Kluwer Academic Publishers, pp 323-343.

2 Kanatas A G, Kountouris I D, Kostaras G B and Constantinou P, A UTD propagation model in urban microcellular environments, 1997, IEEE Trans. Veh. Technol., Vol 46, No 1, pp 185-193.

3 Tan S Y and Tan H S, A microcellular communications propagation model based on the uniform theory of diffraction and multiple image theory, 1996, IEEE Trans. Antennas and Propagat., Vol 44, No 10, pp 1317-1326.

4 Rizk K, Wagen J-F and Gardiol F, Two-dimensional ray-tracing modeling for propagation prediction in microcellular environments, 1997, IEEE Trans. Veh. Technol., Vol 46, No 2, pp 508-518.
5 Zhang W and Lähteenmäki J, UTD-based path loss prediction with experimental validations for micro-cellular mobile radio communications, 1997, Proc. 27th European Microwave Conf., pp 232-237.
6 Kouyoumjian R G and Pathak P H, A uniform geometrical theory of diffraction for an edge in a perfectly conducting surface, 1974, Proc. IEEE, Vol 62, No 11, pp 1448-1461.
7 Zhang W, A more rigorous UTD-based expression for multiple diffractions by buildings, 1995, IEE Proc.-Microw. Antennas Propag., Vol 142, No 6, pp 481-484.
8 Zhang W, A wide-band propagation model based on UTD for cellular mobile radio communications, 1997, IEEE Trans. Antennas and Propagat., Vol 45, No 11, pp 1669-1678.
9 Zhang W, Physical modeling of wide-band propagation for urban line-of-sight micro-cellular mobile and personal communications, 1997, Journal of Electromagnetic Waves and Applications, Vol 11, No 12, pp 1633-1648.
10 Walfisch J and Bertoni H L, A theoretical model of UHF propagation in urban environments, 1988, IEEE Trans. Antennas and Propagat., Vol 36, No 12, pp 1788-1796.
11 Lee S W, Path integrals for solving some electromagnetic edge diffraction problems, 1978, J. Math. Phys., Vol 19, No 6, pp 1414-1422.
12 Saunders S R and Bonar F R, Explicit multiple building diffraction attenuation function for mobile radio wave propagation, 1991, Electron. Lett., Vol 27, No 14, pp 1276-1277.
13 Juan-Llacer L and Cardona N, UTD solution for the multiple building diffraction attenuation function for mobile radiowave propagation, 1997, Electron. Lett., Vol 33, No 1, pp 92-93.
14 Xia H H and Bertoni H L, Diffraction of cylindrical and plane waves by an array of absorbing half-screens, 1992, IEEE Trans. Antennas Propagat., Vol 40, pp 170-177.

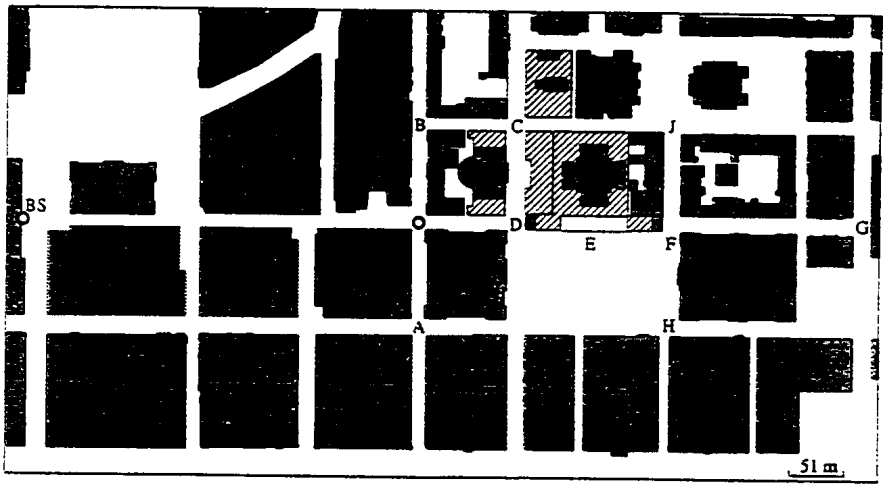


Fig 1: Top view of a street grid of Helsinki city centre, Finland, BS representing Base Station and O indicating its position

Table 1: Measurement system parameters

| parameters | descriptions |
|---|---|
| frequencies | 900.5/1800 MHz |
| polarisation | vertical |
| radiated power $P_t$ | 25 dBm |
| sampling | 1 per 2 meters |
| BS height $h_t$ | 13.3 m |
| BS horn antenna gain | 6.3 dB at 900.5 MHz |
| | 9.2 dB at 1.8 GHz |
| MS relative height $h_r$ | 1.5 m |
| MS antenna type | monopole |

Table 2: Average error $\Delta_{av}$ and root mean square error $\Delta_{rms}$ at 0.9005/1.8 GHz for comparison of 3–D model prediction with measurements in an LOS region

| items | $\Delta_{av}$ (dB) | $\Delta_{rms}$ (dB) |
|---|---|---|
| two–ray | –0.143/–1.05 | 5.25/6.46 |
| four–ray | –0.129/–0.996 | 5.31/6.83 |
| six–ray | –4.55/–6.39 | 7.25/9.67 |
| eight–ray | –4.56/–6.36 | 7.29/9.62 |

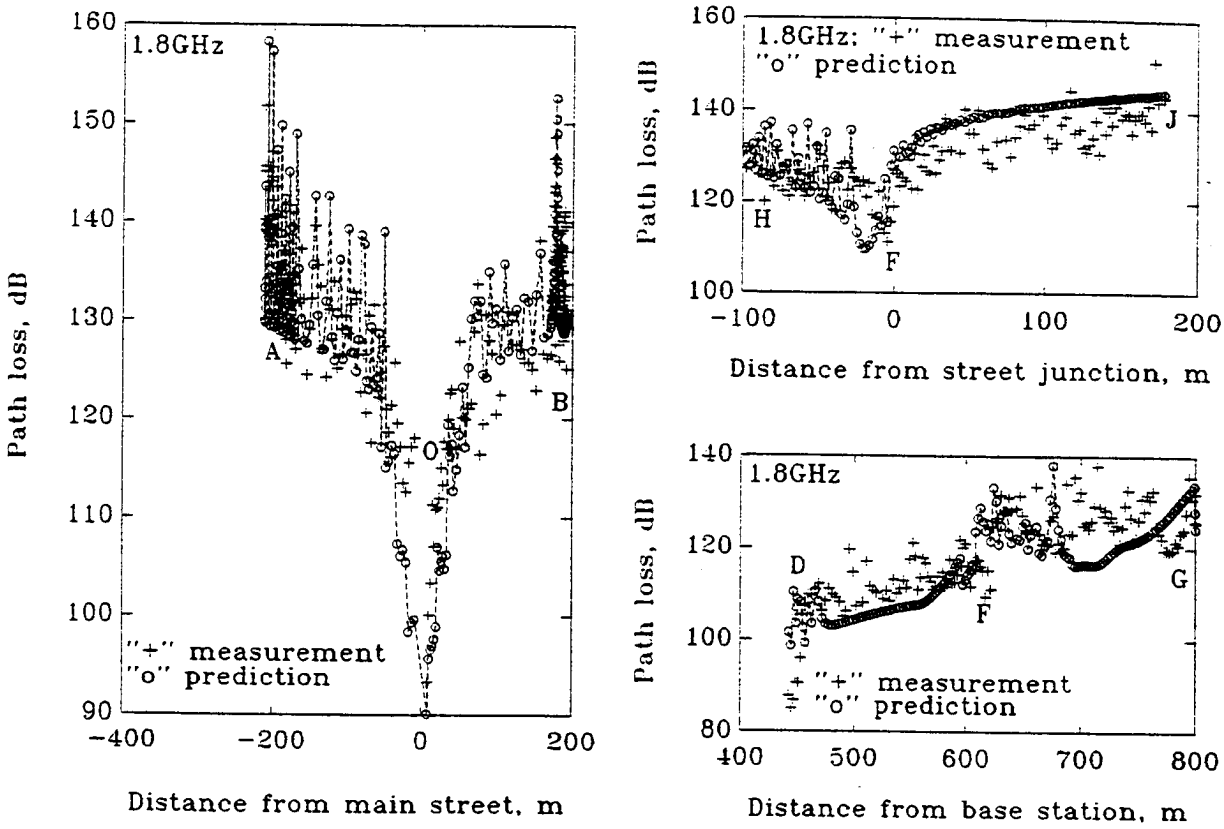


Fig 2: Comparison of model predictions with measurements for side street AOB and for irregular streets HFJ and DEFG of Fig 1

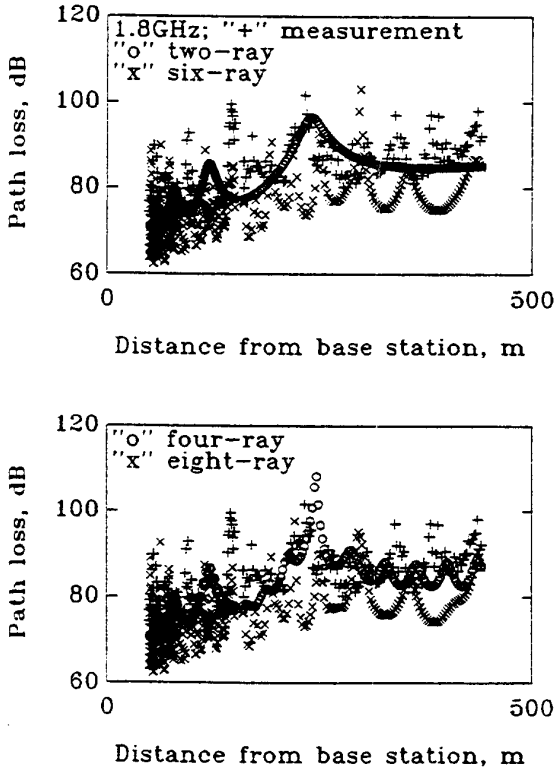


Fig 3: Comparison of model prediction with measurements in an LOS region from BS to D of Fig 1

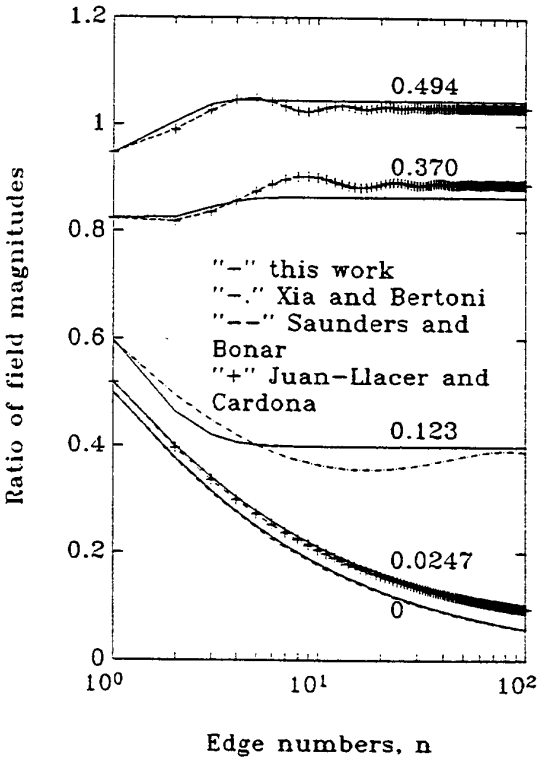


Fig 4: Comparison of the extended formulation for multiple diffraction of hard boundary with existing formulations, grouped by $g$ from 0 to 0.494